Spontaneous Molecular Orientation of Polyimides Induced by Thermal Imidization. 2. In-Plane Orientation

Masatoshi Hasegawa,* Takafumi Matano, Yoichi Shindo, and Tokuko Sugimura

Department of Chemistry, Faculty of Science, Toho University, 2-2-1 Miyama, Funabashi, Chiba 274, Japan

Received January 5, 1996; Revised Manuscript Received July 16, 1996[⊗]

ABSTRACT: The degree of in-plane molecular orientation of various polyimides (PIs) and their precursors, poly(amic acid)s (PAAs), were estimated by measuring the visible dichroic absorption at an incidence angle for a rod-like dye (perylenediimide, PEDI) dispersed in the matrices. The effects of PI chain structure, film thickness, heating rate, and residual solvent on a spontaneous in-plane orientation phenomenon were examined to fully understand the mechanism. All PAA films cast on a substrate showed the low degrees of in-plane orientation of the chain axis, nearly independent of the chain structure. Upon thermal imidization of the PAA films adhered on a substrate, a striking spontaneous in-plane orientation behavior was observed for some PI systems with rigid chains; in contrast to that, some flexible PI systems showed no spontaneous behavior. Cure of the PAA films adhered on a substrate induced the spontaneous orientation even if the films were considerably thick (∼50 μm); in contrast to that, the cure of the free-standing thick film did not. However, upon cure of the free-standing thin films (∼10 μm), the spontaneous orientation behavior was observed. For rigid PI systems in which interchain stacking preferentially occurs, thermal cure of the PAA films on a substrate forms liquid-crystal-like highly oriented regions, and simultaneously, apparent stretching (due to constraint of film contraction during imidization) promotes the molecular orientation further. The mechanism is closely associated with a "cooperative effect" in which the neighboring chains enhance the molecular orientation of each other during cure. In addition, structural changes (orientations of the chain axis and a molecular plane and molecular packing) upon stepwise annealing were followed. Polarized infrared absorption spectra measured at an incidence angle demonstrated that the phthalimide molecular plane in the PI film on a silicon wafer aligns somewhat parallel to the film plane, but no significant orientational and conformational changes occurred upon stepwise annealing.

Introduction

Polyimides have become of interest in recent years for applications as electrical insulators, substrates for flexible printed circuits, passivation layers, and alignment films for liquid crystal displays, owing to their outstanding thermal, mechanical, and dielectric properties. Many studies concerning the structure−property relationship for PI systems have shown that the chemical structure of PI is one of the most important factors associated with the physical properties. For example, roughly speaking, an increase in the PI chain linearity (stiffness) brings about the increases in T_g, modulus, crystallinity, and density and a decrease in thermal expansion coefficient (TEC). According to the point of view, rod-like PMDA−PDA polyimide (PMDA, pyromellitic dianhydride; PDA, *p*-phenylenediamine) is expected to show outstanding properties such as a high modulus and low TEC except for brittleness of the film.

Numata et al.[1−4] demonstrated that to control the TEC of PI films is indispensable to use them as an interlayer electrical insulator and that the PI chain stiffness is the most important factor for this purpose. They also showed that the presence of a metal frame which supports PAA films during imidization (bifix-cure) lowers the TEC of the resulting PI films and inferred that the decreased TEC results from an enhanced molecular orientation. Numerous papers described that the TEC mismatch between a substrate such as Cu and the PI film is responsible for delamination at the interface and cracking in the PI film.[3,5−10]

Recently, a high-temperature annealing method in which aromatic PI films were used as a precursor was developed to obtain a highly crystalline graphite applicable as a monochromator for X-ray analysis. In this method, the high-temperature annealing of PI films cured in a frame provided highly crystalline graphite, whereas that of the films cured free-standing did not.[11−13] The result suggests that the molecular orientation in the PI films as a precursor participates in the mechanism of highly crystalline graphite formation.

In the present paper, "in-plane orientation" represents not molecular orientation within the film plane such as uniaxial orientation, but the degree of the chain axis orientation parallel to the film plane, namely the anisotropy in the edge view. To control TEC, one needs to get a quantitative method for estimating the degree of in-plane molecular orientation of both PAAs and PIs.

The in-plane orientation of PI was first demonstrated by Ikeda.[14] He compared the transmission mode WAXD patterns of the through and edge views for PMDA−ODA (ODA: oxydianiline) polyimide film and illustrated that the former have a reflection peak corresponding to the fiber period stronger than the latter. This proved evidently the presence of in-plane orientation for the crystalline chains. In addition, the PI film sample exhibited a dynamic mechanical loss peak at 80 °C for which the activation energy corresponds to a molecular motion mode of graphite, whereas the molded sample did not. This led him to propose a plane slippage mechanism based on a graphite-like structure.

The in-plane orientation of PMDA−ODA polyimide has been so far studied by means of WAXD,[15,20−27] birefringence measurement with a refractometer or an optical waveguide,[15−19] and reflection infrared spectroscopy.[28] Fortunately, since PMDA−ODA polyimide shows a comparatively sharp reflection peak (002) whose reciprocal lattice vector direction is parallel to the chain

[⊗] Abstract published in *Advance ACS Abstracts,* October 15, 1996.

S0024-9297(96)00018-6 CCC: $12.00

axis, the reflection peak has been frequently used to estimate the molecular orientation of PMDA−ODA. Russel et al.[15] obtained an orientation function by a direct measurement of the integrated intensity of the reflection peak in the edge-view pattern (transmission mode). Instead of taking the edge-view pattern, Takahashi et al.[20] and other groups[21,25,26] compared the transmission and reflection geometrical mode WAXD patterns of PMDA−ODA polyimide films cured on a substrate. From the result in which the transmission mode pattern showed the (002) peak stronger than in the reflection mode, they concluded that the PI chains are in an extended state and align somewhat parallel to the film plane. Similarly, Cheng et al.[22,24] showed that for a fluorinated polyimide derived from 3,3′,4,4′-biphenyltetracarboxylic dianhydride (BPDA) and (2,2′-bis(trifluoromethyl)-4,4′-diaminobiphenyl (TFDB) the (003) reflection peak in the transmission mode pattern is stronger than that in the reflection mode one. Jou et al.[23] demonstrated, by comparing the reflection mode WAXD patterns obtained by the X-ray incidence into the film edge and the film plane, that rod-like PMDA−PDA polyimide chains considerably align relative to the film plane compared with PMDA−ODA polyimide.

The present paper first describes a method for evaluating the degree of in-plane molecular orientation of various PAA and PI chains (from rod-like to flexible) by measuring a visible dichroic spectrum of a rod-like dye dispersed in the matrices[29−32] and focuses on the mechanism of spontaneous orientation of the chain axis. In addition, the orientation of the phthalimide molecular plane with respect to the film plane, estimated by polarized infrared spectroscopy, and structural changes upon stepwise thermal annealing are also described.

We have previously reported that in a semirigid BPDA-PDA polyimide system thermal imidization of the only 50%-drawn PAA film fixed in a metal frame caused the spontaneous uniaxial molecular orientation toward the stretching direction.[33] The result led us to predict that such a spontaneous orientation phenomenon upon thermal imidization might be also observed for unstretched PAA films cast on a substrate; consequently, the polymer chains align parallel to the film plane. The main purpose of this study is to understand the spontaneous in-plane orientation mechanism induced by thermal imidization by examining the effects of the chain stiffness, film thickness, presence of substrate, heating rate, and residual solvent in PAA films.

Experimental Section

Polymeric Materials. PAAs were polymerized by adding the equimolar amount of dianhydride powder into the *N*,*N*-dimethylacetamide (DMAc) or *N*-methyl-2-pyrrolidone (NMP) solutions of diamine with continuous stirring at room temperature for 2 h. The solvents (DMAc and NMP) dried with molecular sieves 4A were distilled under reduced pressure before use.

Molecular structures and symbols of PIs used are listed in Figure 1. The symbols are represented from now on as PI(X/Y), where X and Y denote dianhydride and diamine components, respectively. The abbreviations of monomer components are as follows: pyromellitic dianhydride (PMDA, Tokyo Chemical Industry) (recrystallized from dioxane and then vacuum-dried at 130 °C for 48 h), 3,3′,4,4′-biphenyltetracarboxylic dianhydride (BPDA, Wako Pure Chemical Industries) (vacuum-dried at 200 °C for 24 h), *p*-phenylenediamine (PDA) (recrystallized from ethyl acetate), oxydianiline (ODA) (from toluene/*N*,*N*-dimethylformamide (DMF) (10/1)), *o*-tolidine (OTD) (from benzene), 2,5-dimethyl-*p*-phenylenediamine (DMPDA) (from toluene), *trans*-1,4-cyclohexyldiamine (*t*-CHDA, Aldrich)

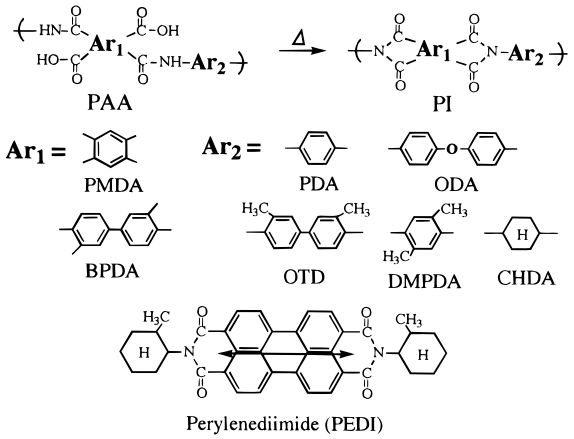

Figure 1. Molecular structures of PAAs, PIs and dichroic dye. The arrow represents the direction of the absorption transition moment of PEDI.

(from hexane). All the diamine monomers recrystallized were vacuum-dried at 40−50 °C for 24 h before use.

PAA solution was cast on a glass plate at 60 °C in an air convection oven with a glass rod or a spin-coater (Mikasa 1H-03) and then cured at 200 °C for 1 h (heating rate: ca. 7 °C min^{-1}) and 250 °C for 1 h in a nitrogen atmosphere (unless indicated otherwise). For preparation of the uniaxially oriented dye-doped PI films, PAA films were first stretched (draw ratio 30%) at room temperatre and then thermally cured in a metal frame.

Poly(vinyl chloride) (Wako Pure Chemical Industries, DP ∼ 1100) was used as an example of flexible polymer without purification.

Dichroic Dye. A dichroic dye, *N*,*N*′-bis(2-methylcyclohexyl)perylenediimide (PEDI), was synthesized from perylenetetracarboxylic dianhydride (PEDA, Tokyo Chemical Industry) and 2-methylcyclohexylamine (MCHA). This reaction occurs with great facility under a condition reported by Langhals et al.:[34,35] PEDA powder (1 g) pre-dried at 200 °C for 24 h was dropped into the dried quinoline solution (25 mL) of a large excess of MCHA ([PEDA]:[MCHA] = 1:20) in the presence of anhydrous zinc acetate as a catalyst (350 mg); then the mixture was vigorously stirred at 180 °C for 4 h. The red precipitate filtered out was washed with 1% NaOH aqueous solution, then ethanol, and finally acetone to remove the unreacted PEDA and residual catalyst. The crude product was recrystallized twice from dimethyl sulfoxide (DMSO), followed by vacuum drying at 180 °C for 24 h. The infrared, visible absorption, and fluorescence spectra of the purified product agreed satisfactorily with those reported in the literature.[34,36,37] Whereas PEDA used as a raw material is quite insoluble in most organic solvents, the product was slightly soluble in several organic solvents, viz., DMAc, NMP, DMSO, tetrahydrofuran, and CH_2Cl_2, and consequently, the solutions showed a strong, yellow fluorescence (fluorescence yield $\Phi_f = 0.91$ in DMAc). Figure 2a shows the visible absorption and the corrected fluorescence spectra of PEDI in DMAc. The dye (PEDA/MCHA) had a solubility higher than the dye obtained from PEDA and cyclohexylamine.

PEDI was quickly dissolved in NMP at 160 °C and cooled to room temperature, and then the solution (1 mL) was mixed vigorously with the DMAc or NMP solution (5 mL) of PAA (10 wt %) (unless indicated otherwise, DMAc solution). After the solution was defoamed under a reduced pressure, the dye-containing solution was immediately cast on a glass plate at 60 °C. The procedure led to the 8−50 μm thick PAA films where the dye is homogeneously dispersed (dye concentration: ca. 2×10^{-3} M). Figure 2b shows the visible absorption spectra of PEDI in PAA(BPDA/PDA) and the corresponding PI films. Although the absorption edge of the matrix itself red-shifts upon imidization, the strong absorption of PEDI peaking at 535 nm allows the selective photoexcitation of the dye.

Both the film samples cured as free-standing samples and in a metal frame were adhered intimately to a glass plate with

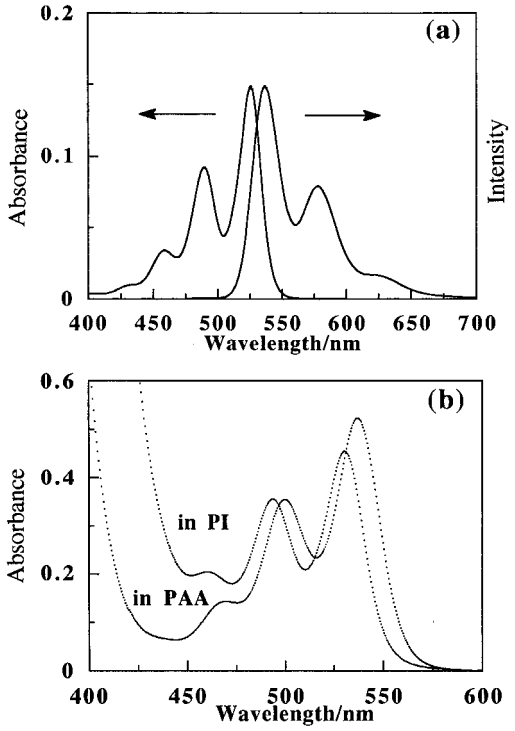

Figure 2. (a) Visible absorption and corrected fluorescence spectra of PEDI in DMAc at room temperature. (b) Visible absorption spectra of the PEDI-containing PAA(BPDA/PDA) and the corresponding PI films at room temperature.

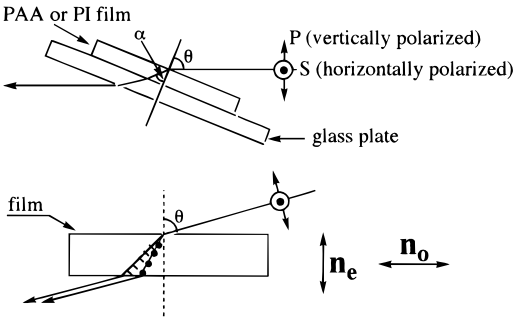

Figure 3. Schematic diagram for dichroic spectrum measurement at an incidence angle.

an adhesive to make the film plane flat for the dichroic spectrum measurements. The absorbance and shape of the absorption spectrum of PEDI in the PI film did not change significantly upon stepwise annealing up to 400 °C (for 10 min at each temperature) in vacuum or nitrogen atmosphere.

Measurements

Evaluation of the Degree of in-Plane Orientation. The degrees of in-plane orientation of PAA and PI chains were estimated by the following procedure: a dye-doped film adhered on a glass plate was irradiated with the monochromatic light beams polarized parallel (P-polarized light) and perpendicular (S-polarized light) to the incidence plane. The absorbance for the P- and S-polarized light beams, A_P and A_S, were measured at an established incidence angle θ at room temperature in an ultraviolet−visible spectrometer (JASCO, Ubest-30) equipped with polarizers (in both the sample and reference sides) mounted between the sample films and the light source. Figure 3 illustrates a schematic diagram of the geometry for the dichroic spectrum measurement. The interference fringes undesirable for dichroic ratio measurement appeared often in the S-polarized absorption spectrum particularly for the spin-coated films. In this case, the fringes were subtracted from the spectrum on a computer. Samples cast with a glass rod, unless noted otherwise, were used for the dichroic spectrum measurements.

For the S-polarized light, the absorbance as a function of the refraction angle, $A_{S\alpha}$, which changes corresponding to the path length change, is expressed independent of the orientational distribution as

$$A_{S\alpha}/A_{S0} = \cos^{-1}\alpha \tag{1}$$

where A_{S0} is absorbance for perpendicular incidence. On the other hand, for the P-polarized light the α-dependent absorbance is expressed in the same form as eq 1 when the orientational distribution is three-dimensionally (3-D) random. By contrast, since the refractive index is generally assumed to have an ellipsoidal form for solvent-cast films, $A_{P\alpha}$ depends on the orientational distribution. In the two-dimensionally (2-D) random (complete in-plane orientation distribution) system, the relation

$$A_{P\alpha}/A_{P0} = \cos\alpha \tag{2}$$

is derived.[38] In the present paper, we define $f = (1 - D)/(1 - D_0)$ as an in-plane orientational parameter, where D ($=A_P/A_S$) is the dichroic ratio which is unity in the case of a three-dimensionally (3-D) random distribution. D_0 ($=\cos^2\alpha$) is the dichroic ratio for the complete in-plane orientation system. Accordingly, the value of f ranges from 0 (3-D random) to unity (2-D random). The f value estimated from the absorption spectra (transmission mode) in this method refers to the degree of in-plane orientation averaged along the thickness direction. The dichroic spectra were measured at θ (57−60° for PAA and PI films used) calculated on the basis of eqs 3 and 4 under the condition of a fixed refraction angle $\alpha = 28°$. If a larger α was used, θ exceeded 60°; consequently, the reflectance increased notably. On the contrary, if too small an α were chosen, the sensitivity lowered.

As shown in Figure 3, the refractive index depends on the polarization direction of the incidence beams (P and S), since PI cast films are generally anisotropic. In this case, for the S-polarized light the refraction phenomenon simply obeys Snell's relation (eq 3). Nevertheless, the refractive index for the P-polarized light is a function of α (ellipsoidal formula) (eq 4).

$$\text{Snell's law} \qquad \sin\theta = n\sin\alpha \qquad (n = n_o \text{ for S-polarized light}) \tag{3}$$

$$n^{-2} = n_o^{-2}\cos^2\alpha + n_e^{-2}\sin^2\alpha \qquad \text{(for P-polarized light)} \tag{4}$$

where n_o and n_e are the refractive indices for the polarized light beams parallel (ordinary) and perpendicular (extraordinary) to the film plane. Prior to the dichroic spectrum measurement, both refractive indices of various PAA and PI films (1 cm × 2 cm) were measured using an Abbe refractometer (Atago 4T, the measurable range: $1.470 < {}^Dn < 1.870$) equipped with a polarizer, sodium lamp (589.3 nm), and test piece ($^Dn = 1.92$). A mixed solution composed of diiodomethane, sulfur, and tin iodide (Atago, $^Dn = 1.800$) was used to keep intimate contact between the main prism, sample film, and test piece. The absorption of all the matrix polymers and PEDI was negligible at the D-line. Some PI films having n_o higher than the ^Dn of the contact solution made the measurement difficult. In this case, the value of n_o was calculated from the measured n_e and the average refractive index n_{av} ($=(2n_o + n_e)/3$) provided by Ando of NTT using the prism coupling technique; $n_{av} = 1.7370$ for PI(PMDA/PDA), 1.7710 for PI(BPDA/PDA), and 1.7284 for PI(BPDA/ODA). The value for PI(BPDA/ODA) agreed well with that obtained with our refractometer.

In a wavelength range where there is no absorption, the refractive indices have generally a tendency to increase with a decrease in wavelength (λ) (normal dispersion) whereas the birefringence change is generally small. The refractive indices at the peak wavelength of PEDI (~535 nm), where the dichroic ratio is taken, does not differ considerably from that measured at the D-line.[10] When incident light is absorbed by a matrix at a wavelength, however, the anomalous dispersion occurs

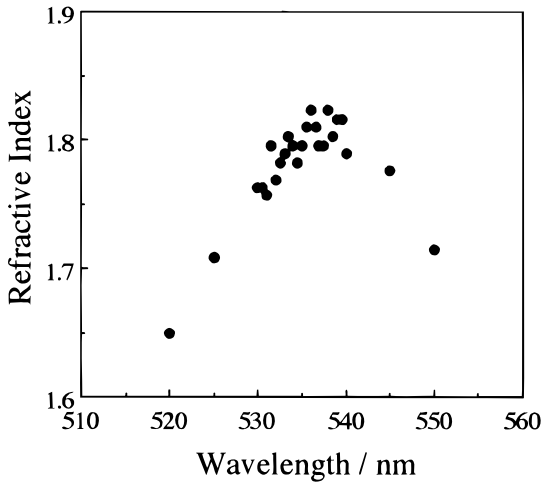

Figure 4. Refractive index dispersion of the PEDI-containing PI(BPDA/PDA) film with respect to the S-polarized light.

in the vicinity of the absorption band. The present method may be subjected to the effect. The refractive index change due to the effect causes the variation in the path length. Then we estimated the anomalous dispersion form as follows: when the spectra are taken at $\theta = 0°$, the path length is not affected by the anomalous dispersion, whereas for the spectra taken at a tilt angle the path length depends on wavelength. In other words, the spectral shape of PEDI in the film for the latter case may be subjected to distortion based on the path length change with λ. For the S-polarized light, eqs 1 and 3 give a refractive index as a function of λ.

$$n(\lambda) = \sin\theta\{1 - [A_{S0}(\lambda)/A_{S\alpha}(\lambda)]^2\}^{-0.5} \quad (5)$$

where $A_{S0}(\lambda)$ denotes absorbance as a function of λ, measured with the S-polarized light at $\alpha = 0°$.

Figure 4 illustrates a refractive index dispersion of the dye-containing PI(BPDA/PDA) film, calculated as $\theta = 60°$ from eq 5. Fortunately, the refractive indices did not sharply vary at the vicinity of the peak position (~535 nm) and were close to the values measured at the D-line on the refractometer, thus indicating that the anomalous dispersion does not practically affect the dichroic ratio measurement at the peak position of PEDI.

The total birefringence of PI films adhered on a substrate is generally represented as the sum of the birefringence contribution due to molecular orientation and residual stress. In the present paper, PI films used for the refractive index measurements are in a free-standing state. On the other hand, the dichroic spectra are taken with PI films remaining on a substrate. Consequently, the latter includes the stress-optical effect. Coburn et al.[10] showed that the birefringence of a PI-(PMDA/ODA) film adhered on a substrate is only 0.004 larger than that of the free-standing PI film (zero-stress birefringence). The difference is much smaller than an error due to the dispersion effects described above. Thus such undesirable optical effects are negligible in this work.

Other Measurements. TECs of PI specimens (15 mm length, 5 mm width, 10−50 μm thickness) were measured on a thermomechanical analyzer (Mac Science, TMA 4010) with a load (0.5 g/1 μm thick) under a nitrogen atmosphere.

PAA(BPDA/PDA) films with varying amounts of residual solvent were prepared by changing the dipping time into water. The amount of residual solvent in PAA films cast from DMAc and NMP were estimated from the extinction coefficient, ϵ, of a specific infrared absorption band of the solvents. The values of ϵ were determined in advance using a NaCl−liquid cell (path length: 0.03 mm) and listed in Table 1. Since the DMAc absorption band overlapped in position with the 1020 cm^{-1} band of the phenylene group in the matrix polymers, the residual DMAc content was obtained by subtracting the 1020 cm^{-1} band absorption. Thermogravimetric analysis (Mac Science, TG-DTA 2000) was conducted in a nitrogen flow to confirm the spectroscopically estimated solvent content and provided the same result as the IR method.

Table 1. Molar Extinction Coefficients and Peak Positions of the Infrared Absorption Bands for NMP and DMAc in CCl_4

	in CCl_4		in PAA film	
solvent	peak/cm^{-1}	ϵ/M^{-1} cm^{-1}	peak/cm^{-1}	ϵ/M^{-1} cm^{-1}
DMAc	1013	82	1020	
NMP	985	34	988	

The densities of PI films were measured at 25 °C using a density gradient column composed of xylene−CCl_4 mixtures. The densities of the PAA(BPDA/PDA) cast film were roughly estimated from the volume and weight to be 1.243 g cm^{-3}, since the residual solvent is removed during the measurement in the column.

The corrected intermolecular charge-transfer (CT) fluorescence spectra of dye-free PI films[39−43] were recorded at room temperature by front-face illumination (excitation, 350 nm; sharp-cut filter, L-39; band-pass, 10 nm (Ex) and 20 nm (Em)) on a Hitachi F-2000 fluorescence spectrometer.

Polarized infrared absorption spectra (transmission mode) for dye-free PI films cast on a silicon wafer were recorded at constant incidence angles of 0 and 60° on a JASCO FT-IR 5300 spectrometer equipped with a KRS-5 polarizer (JASCO PL-81). The variation in the extent of imidization upon stepwise annealing was followed from the absorption ratio of the 1774 cm^{-1} band (imide carbonyl) to the 1515 cm^{-1} (phenyl) band as an internal standard.

Results and Discussion

Effects of Chain Structure on the Degree of in-Plane Orientation. We demonstrated that the PEDI molecule possessing an absorption transition moment directed toward the long molecular axis has a character to align nearly parallel to the PAA and PI chain axis.[33] Ito et al.[44] evaluated the uniaxial orientation toward the dipping direction in a Langmuir−Blodgett film of PI-(BPDA/ODA) by taking the polarized fluorescences of an analogous probe.

For all the dye-doped PAA and PI films, the dichroic absorption ratios taken at $\theta = 0°$ were unity, and additionally, there was no optical birefringence in the film plane, thus indicating that all the film samples were isotropic in the film plane. Figure 5 shows the anisotropy in the edge view, namely, the birefringence Δn ($=n_o - n_e$) as a function of PAA film thickness for PAA(BPDA/PDA) and the corresponding PI films cured on glass. The PAAs exhibited the comparatively low Δn values; nevertheless the PI films showed considerably large birefringence. This leads one to predict that the degree of in-plane orientation increased upon imidization. However, the birefringence data do not always provide a quantitative comparison of molecular orientation unless the intrinsic birefringences Δn_0 of both PAA and PI films are known. The spectroscopic data (dichroism) in combination with the optical data (Δn) enabled us to estimate quantitatively the degree of in-plane molecular orientation independent of the chain structure.

To elucidate the spontaneous in-plane orientation mechanism, we first focus on the effect of polymer chain structure. Parts a−d of Figure 6 illustrate the degree of in-plane orientation, f, of several PAAs, PIs, and PVC. The f value of PVC as a flexible polymer is close to zero, thus indicating nearly 3-D random orientation for PVC.

The PAA films cast from the NMP solution are widely known to contain a large amount of the solvent.[45,46] Nevertheless, the PAAs showed a certain degree of the in-plane orientation, as shown in Figure 6. The result

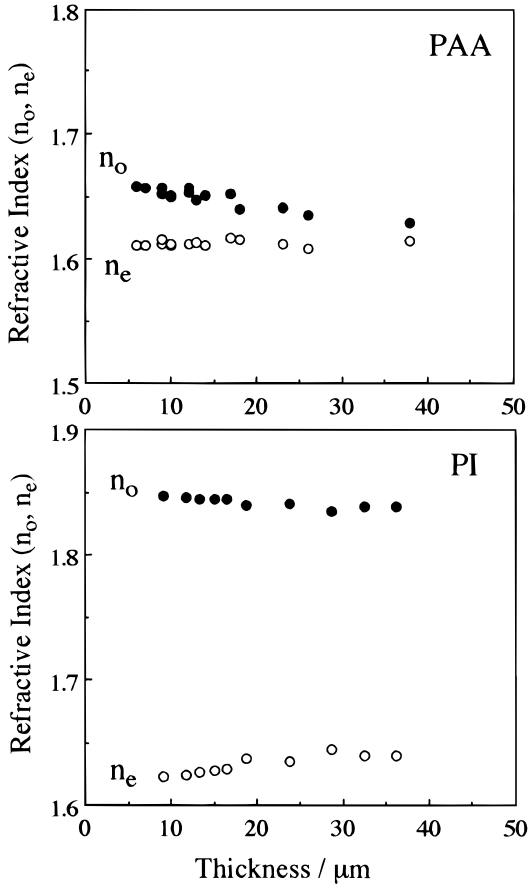

Figure 5. Refractive indices (n_o and n_e) of PAA(BPDA/PDA) and the corresponding PI films cured on a glass plate as a function of PAA film thickness.

is qualitatively consistent with the results derived from the WAXD patterns of PAA(PMDA/ODA) films as illustrated by Takahashi et al.[20] The dependence of f on the chain structure was very small, and the value of f ranged from 0.1 to 0.2 within 10−50 μm for all PAA films. In the stage of PAA, there was unexpectedly no difference of f between flexible BPDA/ODA and rod-like PMDA/PDA systems.

A dimensional change along the thickness direction during solvent evaporation of a polymer solution coated on a substrate probably brings about a certain extent of in-plane orientation. The low f value of PVC demonstrates that the effect of the macroscopic dimensional change during solidification is, however, less efficient for the occurrence of the in-plane orientation. The f values of PAAs higher than those of PVC might result from their chain stiffness and interchain stacking. The initial orientation of PAA film, readily obtained by mere casting onto a substrate, will have an important role for the in-plane orientation enhancement upon thermal imidization.

The PAA coated with a glass rod and the corresponding PI films provided f values no less than for the films prepared through spin-coating. This is probably due to relaxation of a certain extent of orientation generated upon spin-coating during drying at 60 °C. The films prepared with a glass rod are mainly taken from now on.

Note that the degree of in-plane orientation of BPDA/PDA chains enhanced markedly upon thermal imidization of the PAA film adhered on a glass plate without stretching (Figure 6a). The behavior resembles well with the fact that the spontaneous uniaxial orientation

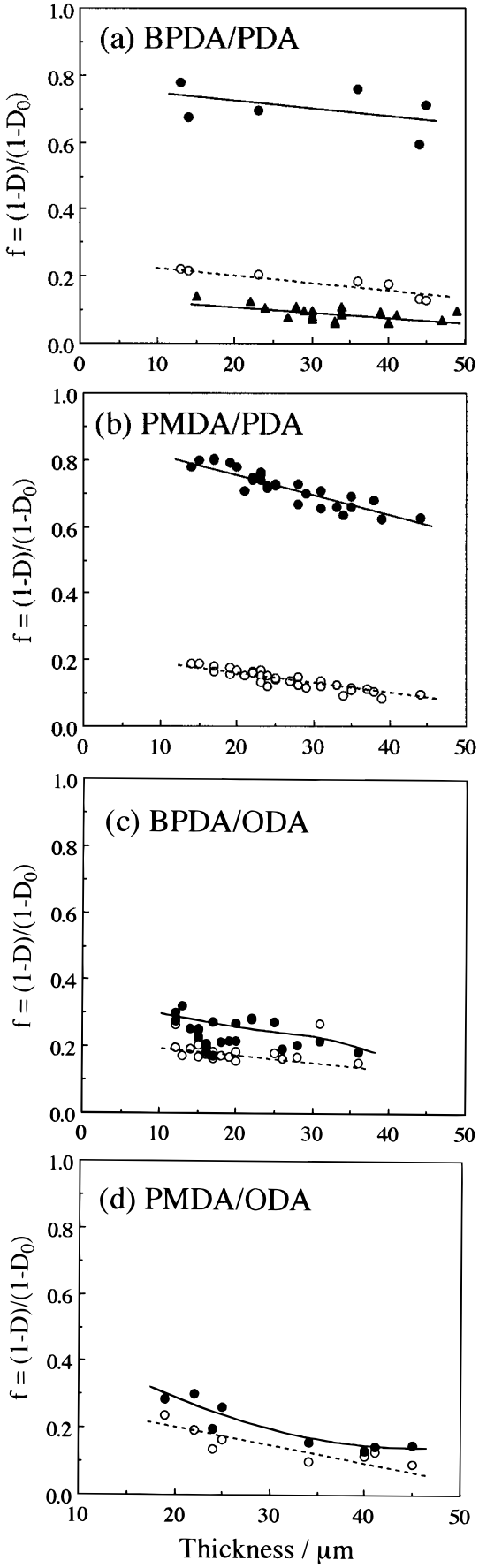

Figure 6. Degree of in-plane orientation for PAAs and the corresponding PI films cured on a glass plate as a function of PAA film thickness: (○) PAA; (●) PI; (▲) PVC.

toward the stretching direction occurred upon thermal imidization of a slightly drawn PAA(BPDA/PDA) film

Table 2. Densities (in g cm^{-3}) of Various PI Films Prepared upon Free-Cure of the 20 μm Thick PAA Films

	dianhydride			
	PMDA		BPDA	
diamine	250 °C	350 °C	250 °C	350 °C
PDA	1.5107		1.4239	1.4615
ODA	1.3807		1.3820	
OTD	1.3281	1.3245	1.3163	1.3149
DMPDA	1.3292	1.3472	1.3015	1.3156
CHDA			1.3406	1.3621

(DR = 50%) supported with a metal frame.[33] The dependence of *f* on film thickness is unexpectedly small, and even in a thicker film (50 μm) a high degree of in-plane orientation was obtained.

For example, the end-to-end distance of a rod-like PI(PMDA/PDA) chain is roughly estimated to be ca. 4.5 μm in the case of DP = 300. This suggests that for such a thick film (50 μm) the PI chain orientation perpendicular to the film plane is not always prevented by the spatial restriction. Namely, imidization itself, which causes a drastic change in the chain linearity, does not result necessarily in the in-plane orientation enhancement. This suggests the existence of strong driving forces for the spontaneous orientation enhancement.

As illustrated in Figure 6b, rod-like PI(PMDA/PDA) showed *f* values a little larger than those of the semirigid BPDA/PDA system. On the other hand, in the BPDA/ODA system possessing the flexible ether linkages in the main chains which lowers considerably the chain linearity, no spontaneous orientation was observed upon curing (Figure 6c). Although PI(PMDA/ODA) containing the ether linkages has been reported to align somewhat parallel to the film plane when the film was cured on a substrate,[15,20] Figure 6d demonstrated evidently that the magnitudes of *f* for PI(PMDA/ODA) are much smaller than those for PMDA/PDA and BPDA/PDA systems. It should be noted, thus, that the strong dependence of *f* for PI films on the chain structure is based on not the difference of the initial PAA chain orientation, but the extent of the spontaneous orientation induced by cure.

As predicted from the result that the degree of spontaneous uniaxial orientation for the BPDA/PDA system increased with increasing draw ratio of the PAA film,[33] the initial in-plane orientation at the PAA stage most likely influences the spontaneous behavior. According to the point of view, the simultaneous biaxial stretching of PAA films is probably an effective way to get highly oriented PI films even for flexible PI systems. The effect of the initial PAA orientation is not addressed in the present work.

Parts a−d of Figure 7 show the degree of in-plane orientation for rod-like PI systems possessing alkyl side groups. PI(PMDA/OTD), in spite of its rod-like chain structure, showed somewhat smaller *f* values than PI(PMDA/PDA) without the bulky substituents. The difference of *f* between these PIs increased with increasing thickness. Comparison of BPDA/OTD and BPDA/PDA systems led to a similar result. It should be noted that no spontaneous behavior was observed in the semirigid BPDA/DMPDA system possessing methyl side groups. These results suggest that there is another important factor for the spontaneous orientation other than the chain stiffness (or linearity).

Table 2 indicates that the film densities of the PIs possessing alkyl substituents are much smaller than those of PIs without the substituents. The lower densities of alkyl-substituted PIs reflect loose interchain stacking. The bulky ortho-substituents (alkyl groups)

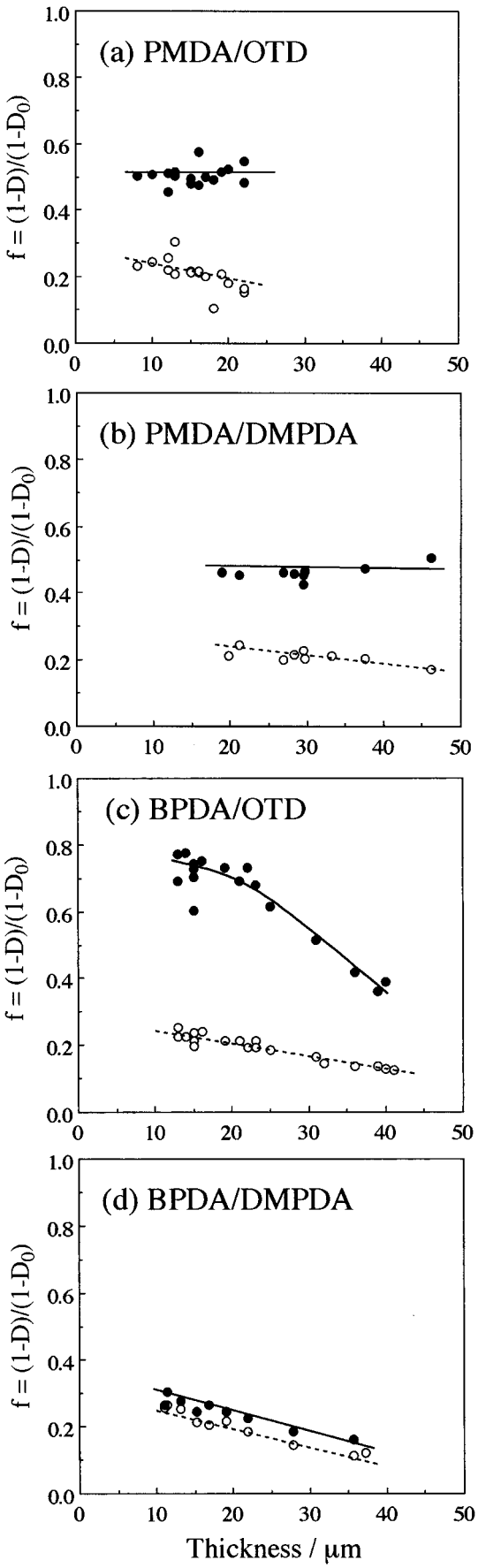

Figure 7. Degree of in-plane orientation for PAAs and PIs possessing alkyl substituents cured on a glass plate as a function of PAA film thickness: (○) PAA; (●) PI.

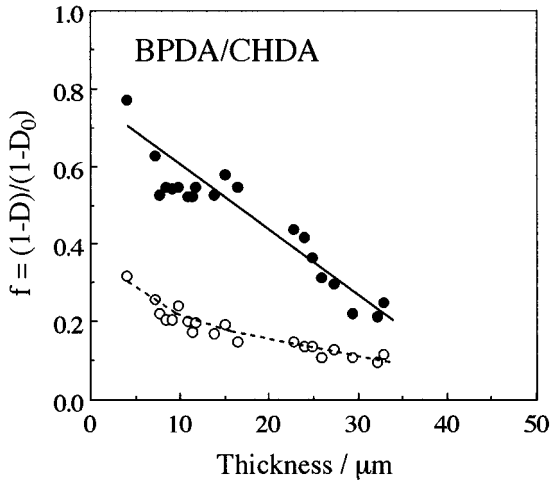

Figure 8. Degree of in-plane orientation for PAA(BPDA/CHDA) (○) and the corresponding PI (●) films cured on glass plate as a function of PAA film thickness.

on the *N*-phenyl group increase the dihedral angle between the phthalimide plane and the phenyl group; consequently, the coplanar structure favorable for dense stacking is destroyed.[47] The loose chain packing most likely results from both steric hindrance to interchain interactions and a decreased molecular motion during cure (hindered internal rotation) due to the presence of the ortho-substituents.

Accordingly, the spontaneous behavior is affected by not only the chain linearity, but also the degree of molecular packing (interchain interactions) during cure and the molecular mobility. In addition, Figure 8 illustrates the in-plane orientation for the semirigid BPDA/CHDA system in which no intermolecular CT interaction exists. The PI films showed a low density (see Table 2), as predicted from its weaker intermolecular interactions.[32] The low degree of spontaneous orientation for thicker films is ascribed to the effect of the intermolecular packing (interactions) on *f* as mentioned above. This problem is discussed later again. To elucidate the spontaneous orientation mechanism, we mainly focus on the BPDA/PDA system which shows the striking spontaneous behavior from now on.

Effect of Substrate. We discuss here an effect of constraint of PAA films during cure on *f*. Thermal imidization brings about a volume decrease of the film owing to evaporation of water as a byproduct and residual solvent. A substrate and frame prevent the film contraction toward the film plane direction; however, these allow contraction along the thickness direction. Figure 9 illustrates the *f* values of PI(BPDA/PDA) cured on a glass plate (substrate-on-cure), cured in a metal frame (bifix-cure), and cured in the free-standing state (free-cure). The bifix-cure samples, of which the *f* values are a little smaller than those of the substrate-on-cure samples, showed the spontaneous orientation obviously. On the other hand, in the free-cure samples *f* decreased abruptly with increasing film thickness; no spontaneous orientation was observed for thicker films (ca. 50 μm). The results support a conclusion of Numata et al.[1] where for a bifix-cured PI(BPDA/PDA) film (40 μm) the value of TEC lower than that of the free-cured film results from not the difference of crystallinity between them but the difference of the degree of in-plane molecular orientation. Thus, Figure 9 indicates evidently that the presence of a substrate or frame plays an important role in inducing the spontaneous orientation.

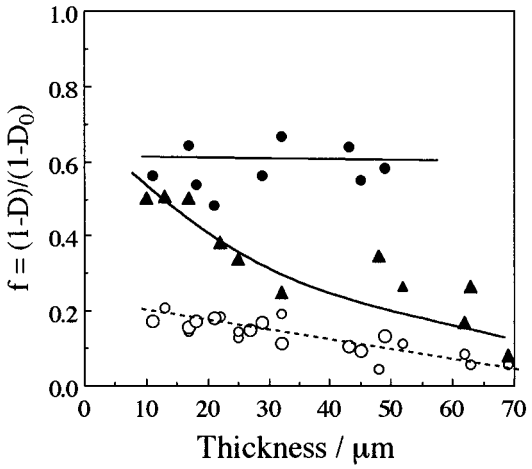

Figure 9. Degree of in-plane orientation for the BPDA/PDA system: (●) PI cured in a metal frame (bifix-cure); (▲) PI cured in the free-standing state (free-cure); (○) PAA films.

Table 3. Dimensional Changes (Thickness (Δt_h), Area (ΔS), and Volume (ΔV)) upon Free- and Bifix-Cure for Various PI Systems

system		t_h (μm)	Δt_h (%)	ΔS (%)	ΔV (%)	f	TEC (ppm)
BPDA/PDA	free	10	20	19	35	0.501	20
	bifix	10	40		40	0.782	6
BPDA/ODA	free	16	0	30	30	0.100	53
	bifix	16	19		19	0.248	32
PMDA/PDA	free	12	50	15	58	0.586	
	bifix	12	42		42	0.790	
PMDA/ODA	free	12	17	34	45	0.162	37
	bifix	12	17		17	0.455	35
PMDA/OTD	free	16	25	9.8	32	0.273	
	bifix	16	50		50	0.330	

Let us consider furthermore the effects of substrate and frame. To prevent the film contraction with a substrate or frame corresponds to an apparent stretching operation toward the film plane direction. Numata et al.[1−4] explained the effect of frame on TEC in terms of the in-plane orientation enhanced by the apparent stretching. Then we examined whether the difference of magnitude of the apparent stretching is responsible for the large difference of the spontaneous behavior observed for various PI systems, as illustrated in Figures 6a−d.

Table 3 summarizes the dimensional decrement (thickness, area, and volume) upon thermal imidization (bifix- and free-cure). For the bifix-cure as well as the substrate-on-cure, the thickness decrease compensates for the inhibition of the area decrease. As shown in Table 3, the thickness decrements (Δt_h) are comparatively high for PMDA/PDA and BPDA/PDA systems which show higher *f* values. On the other hand, for BPDA/ODA and PMDA/ODA giving smaller *f* values the thickness decrements are comparatively low. Thus, there seems to be a correlation of *f* with Δt_h. One would notice, however, that the extent of the apparent stretching estimated from the amount of Δt_h is too small to obtain highly oriented polymer films. A considerably high draw ratio is usually required to enhance markedly the degree of uniaxial orientation of polymer chains: for example, the 400% drawing of PVC film at 95 °C and poly(ethylene terephthalate) specimens at 80 °C provided Herman's orientation functions $F = 0.43$ (ref 48) and 0.75 (ref 49), respectively.

Figure 10 shows the thickness decrement for the BPDA/PDA system (substrate-on-cure) as a function of *f*. The Δt_h was nearly independent of *f*; thus there is

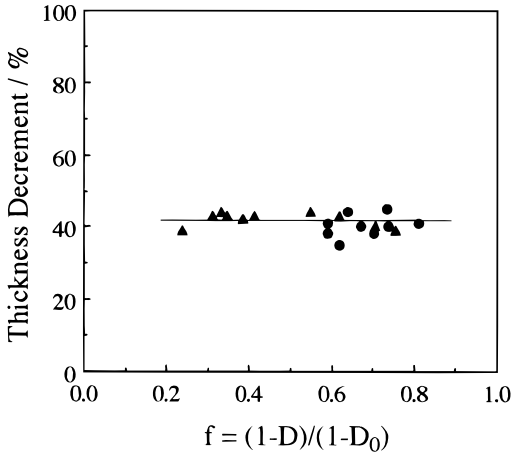

Figure 10. Relation between the degree of in-plane orientation and thickness decrement (%) through thermal imidization for the BPDA/PDA system: (●) films cast from DMAc; (▲) films cast from NMP.

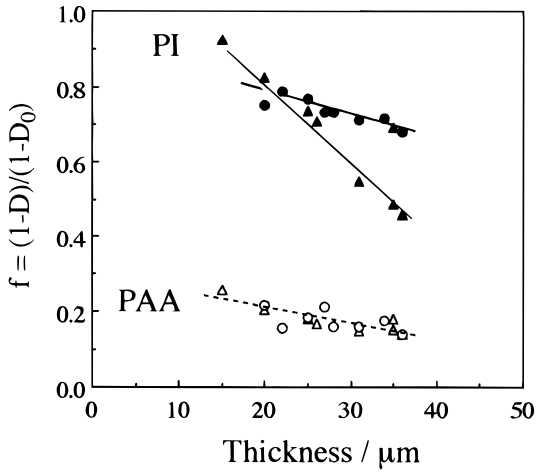

Figure 11. Effect of heating rate on the degree of in-plane orientation of PI(BPDA/PDA) cured on a glass plate: (●) 3 °C min^{-1}; (▲) 7 °C min^{-1}. Open marks represent PAA films.

no relation such that the *f* value increases monotonously with an increase in Δt_h corresponding the extent of apparent stretching. The result excludes an assumption that the macroscopic dimensional change (apparent stretching) upon curing is the direct driving force to give rise to the in-plane orientation of the PI chains.

To discuss the spontaneous orientation mechanism in more detail, we compare the results of thinner and thicker films. As illustrated in Figure 9, for thicker PI films cured in the free-standing state, no spontaneous orientation was observed. On the other hand, the bifix-cure, as well as the substrate-on-cure, enhanced the *f* value markedly even for thicker films. However, the glass/polymer and air/polymer interfaces will not influence the orientation of the polymer chain located in the bulk region for thicker films. What is the driving force for spontaneous behavior observed in thicker films? We propose a mechanism such that liquid-crystal (LC)-like highly oriented regions are formed during thermal cure, and simultaneously, a flow toward the film plane direction caused by the apparent stretching (substrate effect) promotes the orientation of the highly oriented regions. Here, the apparent stretching acts as a kind of trigger. This is probably why the free-cure of thicker films did not give a high degree of orientation.

Factor et al.[27] demonstrated using the grazing incidence X-ray scattering technique that the PI(PMDA/ODA) chains located in the vicinity of the air/polymer interface (70 Å depth from surface) are in extended state much more than those present in bulk ("skin−core" structure). The higher *f* values obtained by the free-cure of the thinner films in contrast to the thicker films as shown in Figure 9 may result from such an air/polymer interface effect. The thinnest film used here (8 μm) is, however, about 1000 times thicker than the thickness of the skin layer (70 Å) where the chains are in an extended state; this suggests that the spontaneous behavior observed in the free-cured thinner films is difficult to explain only in terms of the interface effect.

A kind of PAA is known to form a lyotropic LC state in NMP above a critical concentration.[50,51] In addition, the partially imidized PAA(PMDA/ODA) also shows a LC-like morphology in NMP solution owing to the increased chain stiffness.[51] Thermal cure of a PAA film containing a large amount of solvent will provide molecular motion enough to form the highly oriented regions, but not as large as ones observable with an optical polarized microscope. Such a tendency to form the LC-like structure will become strong with an increase in PI chain stiffness. As mentioned above, we propose the mechanism in which the combination of the formation of the highly oriented regions and the apparent stretching gives rise to the spontaneous orientation even in thicker films. The alkyl substituents on the rod-like PI chains probably disturbs the interchain interaction owing to the steric hindrance. This also acts unfavorably for the formation of LC-like regions. The results of the in-plane orientation of the alkyl-substituted PIs (Figures 6 and 7) are attributable to the substituent effect. In the following, we discuss how molecular mobility affects the in-plane orientation of PI chains.

Effect of Heating Rate. Whereas the degree of molecular packing of PI chains increases upon only local molecular motion, the notable enhancement of the in-plane orientation of the chain axis should need comparatively long distance translational diffusion of the segments. Accordingly, the spontaneous behavior should relate closely with the chain mobility. The rise of heating rate probably brings about an increase in the molecular mobility. Figure 11 shows the dependence of *f* on heating rate (up to 250 °C) for the BPDA/PDA system. For thicker PI films, cure with a low heating rate (3 °C min^{-1}) showed *f* values higher than those cured with a high heating rate (7 °C min^{-1}), although for thinner films there is no difference of *f* between the two heating rates. Thus, the films cured at the higher heating rate have a tendency to be subjected to the orientational relaxation because an increase in heating rate leads to more intensive molecular motion. The result suggests that there exists an optimum heating rate for enhancement of the in-plane orientation; the optimum condition provides adequate molecular mobility necessary for the chain orientation. Note that this differs significantly from the fact that more intensive thermal conditions are favorable for the promotion of local ordering (more dense molecular packing and crystallization) for rigid PI systems.[42]

Effect of Residual Solvent. Brekner and Feger[45,46] demonstrated that PMDA/ODA chains form complexes with residual NMP molecules in the PAA film (the repeating unit: NMP = 1:2 for the PAA film cast at 60 °C) owing to hydrogen bonding. The residual solvent molecules will behave as a plasticizer until the unbound solvent molecules evaporate after decomplexation. For thicker films the solvent molecules stay in the film for

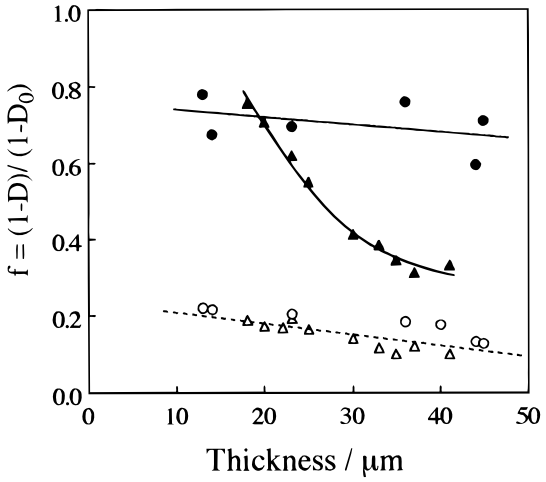

Figure 12. Effect of casting solvent on the degree of in-plane orientation of PI(BPDA/PDA) cured on a glass plate: (●) DMAc; (▲) NMP. Open marks represent PAA films

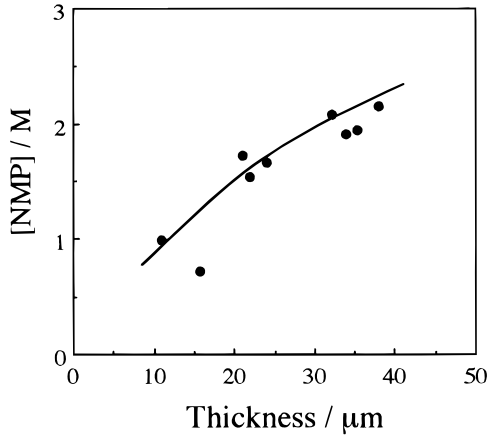

Figure 13. Residual NMP concentration in a PAA film cast from NMP as a function of thickness.

a longer period. As described above, the spontaneous behavior is affected by the chain mobility during thermal cure. Figure 12 shows the effect of the kind of casting solvent on *f*. One might notice that the plots resemble those shown in Figure 11 (the heating rate dependence); the results of the NMP- and DMAc-cast PIs correspond to the results of heating rates of 7 and 3 °C min^{-1}, respectively. NMP is difficult to remove from a PAA film during cure compared with DMAc, as readily predicted from the higher boiling point of NMP. This character of NMP which contributes to an increase in the molecular mobility explains well the effect of solvent on *f* values for thicker films. For NMP-cast films, the dependence of *f* on film thickness can be rationalized by the rate of solvent diffusion from the bulk region to the surface as a function of thickness. In Figure 11, the thickness dependence for the samples cured with 7 °C min^{-1} is probably related with molecular mobility as a function of thickness. The spontaneous orientation behavior is thus dominated by the molecular mobility sensitive to the kind and amount of residual solvent and the heating rate.

Figure 13 exhibits the concentration of residual NMP in a PAA film as a function of film thickness. The solvent concentration increased as the thickness is increased. The thickness dependence of NMP concentration corresponded with the *f* values as a function of thickness, as depicted in Figure 12; the decrease in the *f* value with thickness for the resulting NMP-cast PI

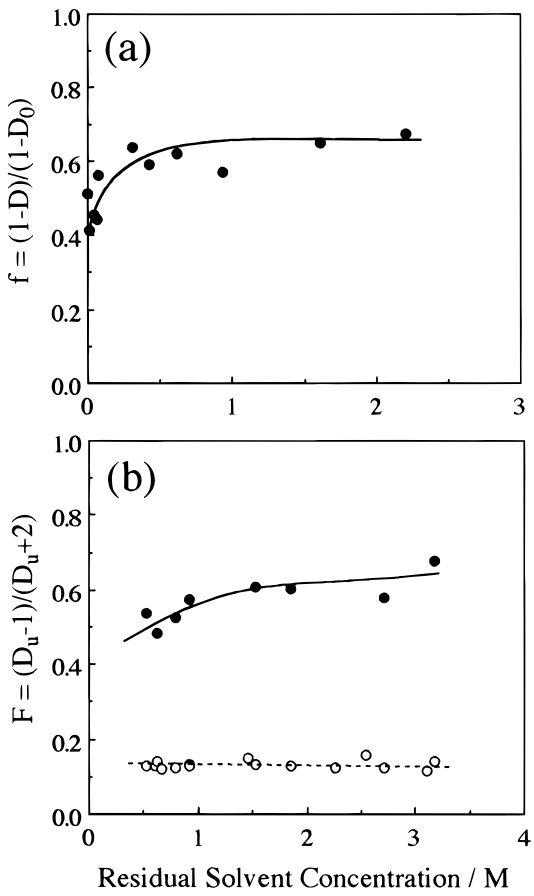

Figure 14. Degree of orientation as a function of the residual DMAc content. (a) Degree of in-plane orientation of PI films free-cured after dipping of the unstretched PAA film (15 μm thick); (b) dichroic orientation function, *F*, of the dipped uniaxially stretched PAA films (17 μm thick, DR = 30%) (○) and the resulting PI films (●).

films can be rationalized in terms of molecular mobility associated closely with the concentration of residual solvent behaving as a plasticizer.

Dipping of the PAA film into water for 0.5 h allowed us to remove almost all of the residual solvent. Since dipping detached PAA film from the substrate, we compared the *f* value of the free-cured PI films prepared from the nondipped and dipped PAA films. Figure 14a demonstrates the variation in the *f* value of the resulting free-cured PI film from the dipped PAA film against the residual DMAc concentration controlled by changing the dipping time; the degree of in-plane orientation decreased somewhat with decreasing solvent concentration. The PI films prepared upon cure of the uniaxially stretched PAA films provided a similar dependence of the dichroic orientation function, $F = (D_u - 1)/(D_u + 2)$ where $D_u = A^{\parallel}/A^{\perp}$, on [DMAc], as shown in Figure 14b. No PAA orientation changed by dipping the stretched PAA films. Thus, the results of Figure 14 combined with Figure 13 led us to conclude that there exists an optimum solvent concentration in PAA films for the in-plane orientation enhancement.

Spontaneous Orientation Behavior of Each Component PI in the Binary Blend System. As reported previously, thermal imidization of the only 50% uniaxially drawn PAA(BPDA/PDA) film supported by a frame caused the notable spontaneous molecular orientation toward the stretching direction, but the flexible BPDA/ODA system exhibited no spontaneous behavior.[33] We prepared PAA(BPDA/PDA) where diamino-PEDI was

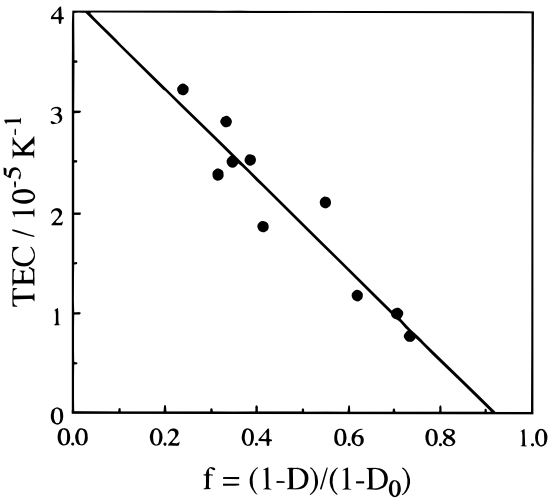

Figure 15. Relationship between the degree of in-plane orientation and TEC of PI(BPDA/PDA) films prepared upon thermal cure (200 °C for 1 h + 250 °C for 1 h on glass) of the NMP-cast PAA films. Prior to TEC measurement, the PI films were annealed at 330 °C for 1 h in free-standing state to remove internal stress.

incorporated in the main chains and examined how much the labeled BPDA/PDA chains align spontaneously upon cure in the unlabeled BPDA/ODA matrix.[52] To suppress transamidation, we prepared the PAA film by immediately casting the vigorously blended solutions for 10 min. The uniaxially stretched binary PAA films supported on a metal frame were thermally cured. The result indicated that the degree of spontaneous uniaxial orientation for the labeled BPDA/PDA chains lowered with increasing BPDA/ODA content in the blend. In the similar blend system composed of unlabeled BPDA/PDA and labeled BPDA/ODA, the flexible BPDA/ODA chains showed the spontaneous orientation somewhat in the BPDA/PDA matrix, whereas the homo BPDA/ODA system is preferentially subjected to the orientational relaxation upon cure. From the fact that this blend system is miscible,[53] the following mechanism is derived: the spontaneous orientation behavior during cure is dominated by not only the chain stiffness but also the interchain interaction, namely, a "cooperative effect" between neighboring chains. When a BPDA/PDA chain was surrounded by flexible BPDA/ODA chains, the spontaneous orientation of the former is hindered by the relaxation tendency of the latter. On the contrary, for the homo BPDA/PDA system the neighboring chains promote each others spontaneous orientation; consequently, a marked orientation behavior is observed. The spontaneous in-plane orientation most likely occurs by the same mechanism. The mechanism described here is not contradictory to the combined mechanism of the formation of highly oriented regions and the apparent stretching, derived in the previous section.

Let us return to the results of Figures 6−8. We mentioned that the interchain stacking is also an important factor for the spontaneous behavior. The lower f values of the alkyl-substituted PIs are interpreted in terms of the loose molecular packing unfavorable for the cooperative effect.

The mechanism of the spontaneous in-plane orientation has been described above. We show here a relation of the degree of in-plane orientation with a physical property. Figure 15 indicates a good reversely proportional relationship between f and TEC for the PI(BPDA/PDA) system. The result means that to fully understand the spontaneous in-plane orientation mechanism is indispensable for the precise control of TEC of PI films.

Structural Changes upon Stepwise Annealing. How does the in-plane orientation occur with the progress of imidization? Parts a−e of Figure 16 show the changes in the extent of imidization (chemical structure) and in physical structures upon stepwise thermal annealing for a BPDA/PDA system (substrate-on-cure). As shown in Figure 16a, thermal imidization of the PAA film adhered on a silicon wafer (4.3 μm thick) begins to occur at 120 °C and almost completes at 250 °C. With an increase in the annealing temperature, the value of f for the PI film (12 μm thick) adhered on a glass plate increased parallel to the progress of imidization and leveled off above 250 °C (Figure 16b). Consequently, additional annealing at higher temperatures for the PI film fully cured at 250 °C led to neither orientational relaxation nor promotion. Similarly, for the uniaxially oriented PI(BPDA/PDA) films cured at 250 °C there was no effect of additional annealing at 330 °C.[33] Figure 16b indicates that the in-plane orientation proceeds only when molecular mobility is available. The lack of chain mobility in a fully cured PI(BPDA/PDA) film is demonstrated by a very small decrease in the dynamic modulus at T_g due to the strong intermolecular interaction.[32,54] A few fluorinated polyimides, i.e., semirigid PI(BPDA/TFDB) and rod-like PI(PMDA/TFDB), which have a comparatively weak intermolecular interaction owing to the presence of the bulky trifluoromethyl substituents, showed the enhancement of molecular orientation and crystallization upon additional annealing of the fully cured PI films above 400 °C.[22,55]

In the same geometry as depicted in Figure 3, the dichroic ratio measurement for a specific infrared absorption band of which the transition moment direction is known provides information on the orientation of a molecular plane (e.g., phthalimide ring) with respect to the film plane. The molecular plane orientation as well as the in-plane orientation of the chain axis must be an important factor for obtaining highly crystalline graphite.[11−13] PI(BPDA/PDA) has several specific absorption bands at 1774 cm^{-1} (ν(C═O) in-phase), 1722 cm^{-1} (ν(C═O) out-of-phase), 1515 cm^{-1} (ν(1,4-phenylene group)), 1340 cm^{-1} (ν(C—N—C)), and 738 cm^{-1} (out-of-plane bending of imide ring).[56] The bands at 1774, 1515, and 1340 cm^{-1} have the parallel dichroic character. Both the 1722 and 738 cm^{-1} bands show the perpendicular dichroism, and the transition moments are parallel (in-plane) for the former and perpendicular (out-of-plane) for the latter to the phthalimide molecular plane.[18,28,56−61]

Figure 16c illustrates the changes in the infrared dichroic ratios measured at $\theta = 60°$ upon stepwise annealing for the PI(BPDA/PDA) film (4.3 μm thick). When the phthalimide molecular plane is in 3-D random orientation, the dichroic ratio takes unity. The 1774 cm^{-1} band showed the dichroic ratios less than unity, indicating evidence of the in-plane orientation of the chain axis. This agrees with the results obtained with the PEDI dye. Other parallel dichroic bands (1515 and 1340 cm^{-1}) also provided dichroic ratios close to those obtained for the 1774 cm^{-1} band. On the other hand, the dichroic ratios for the 738 cm^{-1} band are more than unity in the range 250−400 °C; this means that the phthalimide molecular planes align somewhat parallel to the film plane.

For a very thin film (<100 Å) of PI(PMDA/ODA), reflection infrared spectroscopy demonstrated that

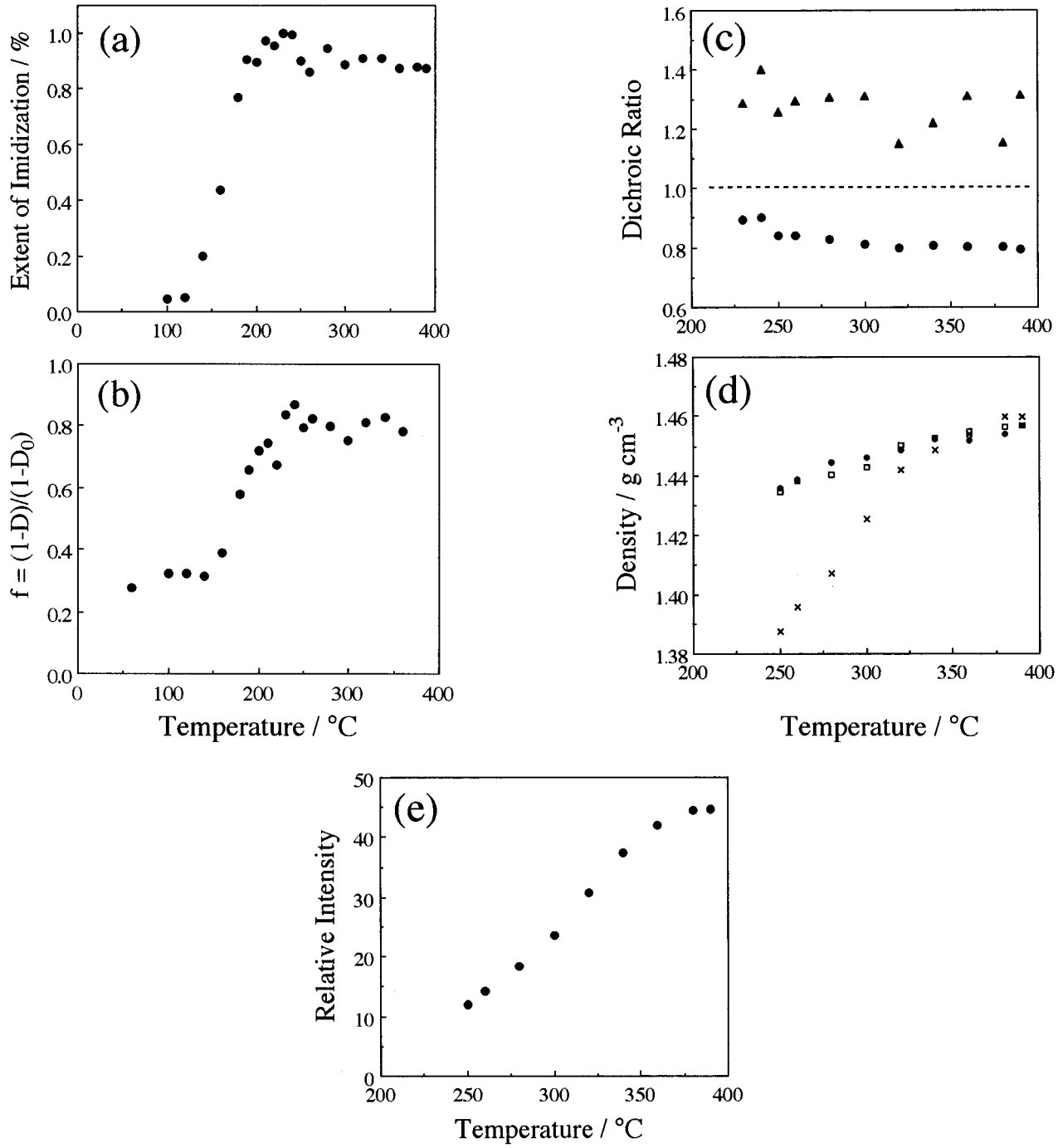

Figure 16. Structural changes of BPDA/PDA during stepwise thermal annealing (10 min at each temperature in a nitrogen atmosphere); (a) the extent of imidization; (b) the degree of in-plane orientation; (c) the dichroic ratios taken at $\theta = 60°$ for the 1774 cm^{-1} band (●) and the 740 cm^{-1} band (▲); (d) densities of PI films (free-cure (×), bifix-cure (□), and substrate-on-cure (●); (e) intermolecular CT fluorescence intensity (substrate-on-cure). For (c−e), the films were annealed on the same thermal program as (a) and (b).

both the chain axis and the pyromellitimide molecular plane align somewhat with the film plane.[28] However, for the films thicker than 150 Å the pyromellitimide plane orientation becomes isotropic completely, although the in-plane orientation of the chain axis still remains. It is noteworthy that the orientation of phthalimide planes in the PI(BPDA/PDA) film was observed even in a much thicker film (4.3 μm thick). No significant changes in the dichroic ratios for both bands occurred through stepwise annealing, as shown in Figure 16c. Thus, the phthalimide molecular plane orientation in the PI(BPDA/PDA) film is not affected by the stepwise annealing at higher temperatures as well as the chain axis in-plane orientation.

The peak position change of a few specific infrared absorption bands (measured at $\theta = 0°$) were also followed on stepwise annealing process. According to Ishida et al.,[62] a decrease in the dihedral angle between the phthalimide plane and *N*-phenyl group, which intensifies the conjugation, causes the peak shift toward higher wavenumber for the bands peaking at 1515 and 1380 cm^{-1}. The stepwise annealing at higher temperatures exhibited no peak shift for both bands, thus suggesting that no significant conformational changes around the *N*-phenyl linkage occurred.

Parts d and e of Figure 16 show the changes in density and in the intermolecular CT fluorescence intensity I_{CT}, respectively. With an increase in anneal-

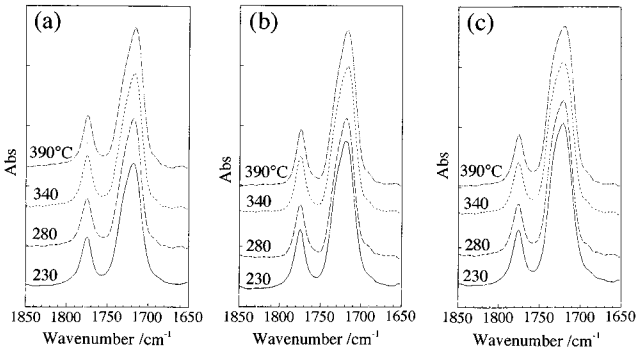

Figure 17. Polarized and unpolarized infrared absorption spectra of the PI(BPDA/PDA) film cured at 250 °C on a silicon wafer: (a) $\theta = 0°$, unpolarized; (b) $\theta = 60°$, S-polarized light; (c) $\theta = 60°$, P-polarized light.

ing temperature, both density and I_{CT} increased gradually. The substrate-on-PI films showed densities higher than the free-cured films, indicating the more dense molecular packing for the former. The CT fluorescence is based on the CT complexes intermolecularly formed on face-to-face overlap between an electron donor (diamine moiety) and acceptor (diimide moiety) in the PI chains. The dense interchain stacking results in an increase in the CT complex concentration, and as a result, the CT fluorescence intensity increases.[39−43] Accordingly, the result indicates an increase in the degree of molecular packing (local ordering) upon annealing. In addition, we found that growing and splitting of several infrared absorption bands (<1000 cm^{-1}) are caused by annealing at 400 °C, attributed to the local molecular ordering,[63] which will be reported in a separate paper in detail. Thus, the local ordering in the BPDA/PDA system proceeds favorably by annealing at a higher temperature, in contrast to the results that the orientation of the chain axis and the phthalimide molecular plane and the conformation around the *N*-phenyl linkage are not affected by the stepwise higher temperature annealing. This is probably due to the degree of molecular packing readily increasing with only local molecular motion.

Another important point to note in the difference of the annealing effect on the orientation and the molecular packing (ordering) is that more intensive molecular motion (severe annealing condition) acts favorably for the molecular packing, whereas it is unfavorable for the orientation (orientational relaxation is predominant). That is, there is an optimum annealing condition for molecular mobility to enhance the in-plane orientation, as described above.

Parts a−c of Figure 17 display the polarized and unpolarized infrared absorption spectra of the 1722 cm^{-1} band measured at $\theta = 0$ and 60° as a function of annealing temperature for the PI(BPDA/PDA) film. If the band were composed of one component, no anisotropy for the spectral shape should be observed. The spectrum measured at $\theta = 0°$ is similar in shape to the S-polarized absorption spectrum measured at $\theta = 60°$, but at $\theta = 60°$ the S-polarized spectrum differs significantly from the P-polarized spectrum. In contrast to that the spectral shape of the 1774 cm^{-1} band is independent of the polarization direction. A shoulder appeared around 1740 cm^{-1} in the P-polarized spectrum. The higher (1740 cm^{-1}) and lower (1722 cm^{-1}) frequency bands were assigned as the imide-carbonyl asymmetric stretching for the PI chains located in the less ordered and ordered regions, respectively.[18,56] Under the assumption that the transition moment direction of both bands is the same, the comparison of the S-polarized and the P-polarized spectra indicates that the PI chains oriented in the film plane include the higher fraction of the chains located in the ordered regions, compared with the unoriented PI chains. In addition, the effect of stepwise annealing temperature on the spectral shape was not so marked in this system.

Conclusions

The effects of chain stiffness, substrate, heating rate, and residual solvent were investigated by estimating the degree of in-plane orientation of the chain axis from the dichroic ratio of PEDI dye. The results led us to propose a mechanism for the spontaneous in-plane orientation induced by thermal imidization as follows: for PI systems with more rigid chains, liquid-crystal-like highly oriented regions are formed in the film during cure, and simultaneously, the apparent stretching caused by a substrate or frame promotes the orientation of the highly oriented regions further. This mechanism is closely associated with the cooperative effect where the neighboring chains enhance the orientation of each other during cure.

Upon stepwise annealing, the degree of in-plane orientation of the chain axis increases parallel to the progress of imidization and levels off above 250 °C where cure is complete. Accordingly, a certain extent of molecular mobility is required for the enhancement of the in-plane orientation. On the other hand, the degree of molecular packing increases upon stepwise annealing of the fully cured PI film even if no intensive molecular mobility is available. There is an optimum annealing condition influencing the molecular mobility to bring about the spontaneous orientation; in contrast to that more intensive molecular motion (severe thermal condition) is favorable for enhancement of the molecular packing (ordering).

The phthalimide molecular planes align somewhat parallel to the film plane. However, the orientation of the chain axis, the molecular plane, and conformation around the *N*-phenyl linkage did not change significantly upon the stepwise annealing at higher temperatures for the fully cured PI film.

Acknowledgment. We thank Dr. S. Ando of NTT and Dr. T. Miwa of Hitachi Ltd. for their useful comments.

References and Notes

(1) Numata, S.; Oohara, S.; Fujisaki, K.; Imaizumi, J.; Kinjo, N. *J. Appl. Polym. Sci.* **1986**, *31*, 101.
(2) Numata, S.; Fujisaki, K.; Kinjo, N. *Polymer* **1987**, *28*, 2282.
(3) Numata, S.; Kinjo, N.; Makino, D. *Polym. Eng. Sci.* **1988**, *28*, 906.
(4) Numata, S.; Miwa, T. *Polymer* **1989**, *30*, 1170.
(5) Elsner, G. *J. Appl. Polym. Sci.* **1987**, *34*, 815.
(6) Nomura, H.; Eguchi, M.; Asano, M. *J. Appl. Phys.* **1991**, *70*, 7085.
(7) Jou, J. H.; Chung, C. S. *Macromolecules* **1992**, *25*, 6035.
(8) Ree, M.; Nunes, T. L.; Czornyj, G.; Volksen, W. *Polymer* **1992**, *33*, 1228.
(9) Pottiger, M. T.; Coburn, J. C.; Edman, J. R. *J. Polym. Sci., Part B* **1994**, *32*, 825.
(10) Coburn, J. C.; Pottiger, M. T.; Noe, S. C.; Senturia, S. D. *J. Polym. Sci., Part B* **1994**, *32*, 1271.
(11) Murakami, M.; Nishiki, N.; Nakamura, K.; Ehara, J.; Okada, H.; Kouzaki, T.; Watanabe, K.; Hoshi, T.; Yoshimura, S. *Carbon* **1992**, *30*, 255.
(12) Hatori, H.; Yamada, Y.; Shiraishi, M. *Carbon* **1992**, *30*, 763.
(13) Inagaki, M.; Sato, M.; Takeichi, M.; Yoshida, A.; Hishiyama, Y. *Carbon* **1992**, *30*, 903.

(14) Ikeda, R. M. *J. Polym. Sci., Polym. Lett. Ed.* **1966**, *4*, 353.
(15) Russel, T. P.; Gugger, H.; Swalen, J. D. *J. Polym. Sci., Polym. Phys. Ed.* **1983**, *21*, 1745.
(16) Nakagawa, K. *J. Appl. Polym. Sci.* **1990**, *41*, 2049.
(17) Herminghaus, S.; Boese, D.; Yoon, D. Y.; Smith, B. A. *Appl. Phys. Lett.* **1991**, *59*, 1043.
(18) Boese, D.; Lee, H.; Yoon, D. Y.; Swalen, J. D.; Rabolt, J. F. *J. Polym. Sci.: Part B* **1992**, *30*, 1321.
(19) Ree, M.; Chu, C. W.; Goldberg, M. J. *J. Appl. Phys.* **1994**, *75*, 1410.
(20) Takahashi, N.; Yoon, D. Y.; Parrish, W. *Macromolecules* **1984**, *17*, 2583.
(21) Coburn, J. C.; Pottiger, M. T. *Proceedings of 4th Conference on Polyimides*; Technomic: Lancaster, PA, 1991; p 360.
(22) Cheng, S. Z. D.; Arnold, F. E., Jr.; Zhang, A.; Hsu, S. L. C.; Harris, F. W. *Macromolecules* **1991**, *24*, 5856.
(23) Jou, J. H.; Huang, P. T.; Chen, H. C.; Liao, C. N. *Polymer* **1992**, *33*, 967.
(24) Arnold, .F. E., Jr.; Shen, D.; Lee, C. J.; Harris, F. H.; Cheng, S. Z. D.; Lau, S. F. *J. Mater. Chem.* **1993**, *3*, 353.
(25) Goeschel, U.; Lee, H.; Yoon, D. Y.; Siemens, R. L.; Smith, B. A.; Volksen, W. *Colloid Polym. Sci.* **1994**, *272*, 1388.
(26) Ree, M.; Nunes, T. L.; Lin, J. S. *Polymer* **1994**, *35*, 1148.
(27) Factor, B. J.; Russell, T. P.; Toney, M. F. *Macromolecules* **1993**, *26*, 2847.
(28) Perez, M. A.; Ren, Y.; Farris, R. J.; Hsu, S. L. *Macromolecules* **1994**, *27*, 6740.
(29) Hasegawa, M.; Matano, T.; Shindo, Y.; Sugimura, T. *J. Photopolym. Sci. Technol.* **1994**, *7*, 275.
(30) Hasegawa, M.; Matano, T.; Shindo, Y.; Sugimura, T. In *Polymeric Materials for Microelectronic Applications*; Ito, H., Tagawa, S., Horie, K., Eds.; ACS Symposium Series 579, American Chemical Society: Washington, DC, 1994; p 234.
(31) Hasegawa, M; Matano, T.; Shindo, Y.; Sugimura, T. In *Polyimides: Trends in Materials and Applications*; Feger, C., Khojasteh, M. M., Molis, S. E., Eds.; Society of Plastics Engineers: New York, 1996; p 239.
(32) Hasegawa, M.; Isii, J.; Matano, T.; Shindo, Y.; Sugimura, T.; Miwa, T.; Ishida, M.; Okabe, Y.; Takahashi, A. In *Microelectronics Technology: Polymers for Advanced Imaging and Packaging*; Reichmanis, E., Ober, C. K., MacDonald, S. A., Iwayanagi, T., Nishikubo, T., Eds.; ACS Symposium Series 614; American Chemical Society: Washington, DC, 1995; p 395.
(33) Hasegawa, M.; Shindo, Y.; Sugimura, T.; Yokota, R.; Kochi, M.; Mita, I. *J. Polym. Sci., Part B* **1994**, *32*, 1299.
(34) Rademacher, A.; Markle, S.; Langhals, H. *Chem. Ber.* **1982**, *115*, 2927.
(35) Langhals, H. *Chem. Ber.* **1985**, *118*, 4641.
(36) Ford, W. E.; Kamat, P. V. *J. Phys. Chem.* **1987**, *91*, 6373.
(37) Nagao, Y.; Misono, T. *Bull. Chem. Soc. Jpn.* **1981**, *54*, 1191.
(38) Wolf, E. *Progress in Optics XII*; North-Holland: Amsterdam, 1974; p 189.
(39) Wachsman, E. D.; Frank, C. W. *Polymer* **1988**, *29*, 1191.
(40) Hasegawa, M.; Mita, I.; Kochi, M.; Yokota, R. *J. Polym. Sci., Part C* **1989**, *27*, 263.
(41) Hasegawa, M.; Kochi, M.; Mita, I.; Yokota, R. *Eur. Polym. J.* **1989**, *25*, 349.
(42) Hasegawa, M.; Arai, H.; Mita, I.; Yokota, R. *Polym. J.* **1990**, *22*, 875.
(43) Hasegawa, M.; Mita, I.; Kochi, M.; Yokota, R. *Polymer* **1991**, *32*, 3225.
(44) Ito, S.; Kanno, K.; Ohmori, S.; Onogi, Y.; Yamamoto, M. *Macromolecules* **1991**, *24*, 659.
(45) Brekner, M. J.; Feger, C. *J. Polym. Sci., Part A* **1987**, *25*, 2005.
(46) Brekner, M. J.; Feger, C. *J. Polym. Sci., Part A* **1987**, *25*, 2479.
(47) Hasegawa, M.; Sonobe, Y.; Shindo, Y.; Sugimura, T.; Karatsu, T.; Kitamura, A. *J. Phys. Chem.* **1994**, *98*, 10771.
(48) Ohmori, S.; Ito, S.; Onogi, Y.; Nisijima, Y. *Polym. J.* **1987**, *19*, 1269.
(49) Bower, D. I.; Korybut-Daszkiewicz, K. K. P.; Ward, I. M. *J. Appl. Polym. Sci.* **1983**, *28*, 1195.
(50) Whang, W. T.; Wu, S. C. *J. Polym. Sci., Part A* **1988**, *26*, 2749.
(51) Huang, J. W.; Chu, N. J. *J. Chin. Inst. Chem. Eng.* **1991**, *22*, 45.
(52) Hasegawa, M.; Horimoto, M.; Matano, T.; Shindo, Y.; Sugimura, T.; Yokota, R.; Kochi, M. *Polym. Prepr. Jpn.* **1995**, *44*, 583.
(53) Yokota, R.; Horiuchi, R.; Kochi, M.; Soma, H.; Mita, I. *J. Polym. Sci., Part C* **1988**, *26*, 215.
(54) Kochi, M.; Uruji, T.; Iizuka, T.; Mita, I.; Yokota, R. *J. Polym. Sci., Part C* **1987**, *25*, 441.
(55) Ando, S.; Sawada, T.; Inoue, Y. In *Polymeric Materials for Microelectronic Applications*; Ito, H.; Tagawa, S., Horie, K., Eds.; ACS Symposium Series 579; American Chemical Society: Washington, DC, 1994; p 283.
(56) Ishida, H.; Wellinghoff, S. T.; Baer, E.; Koenig, J. L. *Macromoleculaes* **1980**, *13*, 826.
(57) Laius, L. A. *Vysokomol. Soedin.* **1974**, *A16*, 2101; *Polym. Sci. USSR* **1974**, *16*, 2435.
(58) Snyder, R. W.; Sheen, C. W.; Painter, P. C. *Appl. Spectrosc.* **1988**, *42*, 503.
(59) Molis, S. E. In *Polyimides: Materials, Chemistry and Characterization*; Feger, C., Khojasteh, M. M., McGrath, J. E., Eds.; Elsevier: Amsterdam, 1989; p 659.
(60) Pryde, C. A. *J. Polym. Sci., Part A* **1989**, *27*, 711.
(61) Pryde, C. A. *J. Polym. Sci., Part A* **1993**, *31*, 1045.
(62) Ishida, H.; Huang, M. T. *J. Polym. Sci., Part B* **1994**, *32*, 2271.
(63) Vladimirov, L.; Hasegawa, M.; Yokota, R. *Polym. Prepr. Jpn.* **1995**, *44*, 588.

MA960018N